4th International Conference on Molten Slags and Fluxes, 1992, Sendai, ISIJ

INCLUSION TRANSFER BEHAVIOR ACROSS MOLTEN STEEL-SLAG INTERFACE

Keiji Nakajima and Kazuo Okamura

Iron and Steel Research Laboratories, Sumitomo Metal Industries, Ltd., Japan

Synopsis: To investigate the critical condition of inclusion elimination, the dynamic behavior of a rising inclusion across the molten steel-slag interface was studied theoretically. An effective and simple model which predicts the rate and displacement of inclusion was proposed. It was postulated in the model that the behavior of inclusion elimination is composed of several steps: a preliminary approach, a steel film thinning (drainage), a steel film rupture and a contact with the slag. A theoretical analysis based on the above model was developed by considering the buoyancy force, the drag force, the fluid added mass force and the rebound force due to the interfacial energy change. The numerical results agree quantitatively with previous simulation-experimental results.

Key words: inclusion elimination, slag viscosity, wettability, interfacial tension, steel film

1. Introduction

The elimination of inclusions has recently become a subject of special interest. In the continuous casting process, it is extremely important to stably and quickly eliminate large quantities of inclusions. However, the mechanism of inclusion elimination is not yet fully understood, and there are a number of unsolved problems regarding the elimination of inclusions because of the complicated process.

In this paper, the hydrodynamic mechanism of inclusion elimination in steel-slag-inclusion systems has been studied. It is important to clarify this phenomenon using theoretical analysis because of the difficulty of correctly measuring the dynamic behavior of inclusion elimination. There have been a few theoretical [1～6] and simulation-experimental [7～9] reports on the moving body across the interface. However, these studies do not deal with inclusion with steel film and are based on qualitative discussion. Since the present phenomenon is related closely to the dynamic instability of interface and the rupture of steel film, an effective theory of inclusion elimination was developed here by considering slag viscosity, wettability and the dynamic motion of an inclusion across the interface. The numerical results based on this analysis agreed quantitatively with previous simulation-experimental data. The results obtained here will provide useful suggestions for future research and the development of inclusion elimination.

2. Theoretical Approach

2.1 Theoretical model

As described in section 1, it is important for the estimation of inclusion elimination to analyze the dynamic behavior of the rising inclusion across the interface. Thus, a model that distinguishes two types of behavior when inclusions cross the interface was proposed, as demonstrated schematically

in Fig. 1(a), (b). Z is the displacement of the inclusion center from the standard point (Z=0) which is located at the distance of the inclusion radius R_I from the stationary horizontal interface. The Z-direction is the opposite of that of gravity g. Time t starts from zero when the center of inclusion reaches the standard point. P is pressure and subscripts r and θ denote the r- and θ-directions, respectively, where (r, θ) is the spherical polar coordinates with an axial symmetry, and S is the film thickness. The theoretical analysis was developed under the following assumptions.

(1) The inclusion is spherical. The inclusion volume does not change as the inclusion moves across the interface. That is, the inclusion is insoluble in slag.

(2) The fluids are incompressible and isothermal.

The steel film formation occurs in the range $Re_{I\langle 0\rangle} \geqq 1$. In this case, the additional assumptions are given as follows.

(3) The steel film has a concentric spherical shape. The film thickness is uniform along the inclusion surface and extremely thin. The r-direction flow in the film is negligibly small.

(4) The flow around the inclusion is expressed as follows.

$$\phi = -(1/2)\cdot dZ/dt\cdot \{(-3/2)rR_I + (1/2)R_I^3/r\}\cdot \sin^2\theta \tag{1}$$

Here, ϕ is the stream function. This equation is used in the ranges $r \geqq R_I$ and $0 \leqq \theta \leqq \pi$. The drag coefficients Cd_M, Cd_S of the inclusion derived from Eq. (1) are $24/Re_M$, $24/Re_S$, respectively.

(5) The interface tension is uniform. Since the pressure P_S near the interface varies little during deforming of the interface due to the small inclusion, P_S equals P_M approximately. From these simplifications and Eq. (1), the continuity of normal stress across the steel film-slag interface is expressed as follows [6].

$$P_F - P_S \fallingdotseq P_F - P_M = 2\sigma_{MS}/(R_I+S) + (dZ/dt)\cdot 2\mu_S\cdot(3/2)\ \{1/(R_I+2S) - 1/(R_I+4S)\}\cdot\cos\theta \tag{2}$$

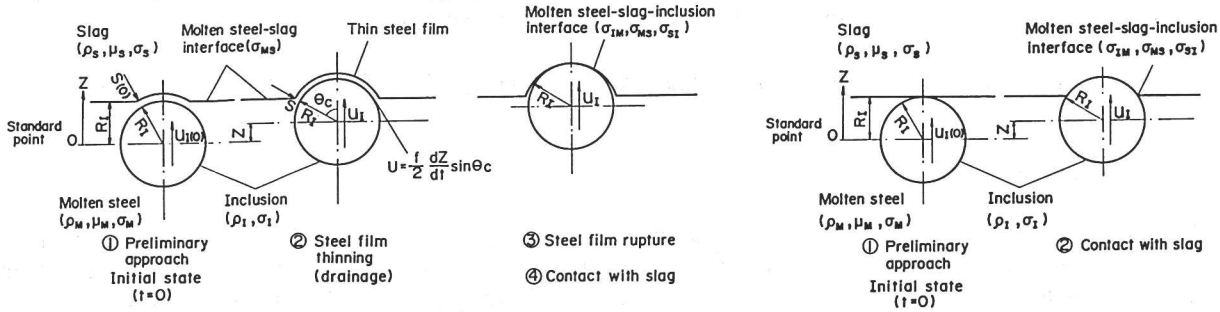

Fig. 1. Schematic representation of two types of behavior when inclusions cross the interface.

2.2 Dynamic force on inclusion

2.2.1 Inclusion with steel film

In this section, the dynamic force on inclusion with steel film is first described. Secondly, the rate of film drainage is explained. The rebound force Fr is obtained from Eq. (2) as follows.

$$\begin{aligned} Fr &= \int (P_F - P_M)\cos\theta\,(2\pi R_I \sin\theta)R_I\,d\theta \\ &= 4\pi R_I^2\,[\,\{\sigma_{MS}/(2(R_I+S))\}\cdot\sin^2\theta_c \\ &\quad + (dZ/dt)\cdot(\mu_S/3)\cdot(3/2)\ \{1/(R_I+2S) - 1/(R_I+4S)\}\cdot(1-\cos^3\theta_c)\,] \end{aligned} \tag{3}$$

The buoyancy force Fb, the drag force Fd and the fluid added mass force Ff due to the accelerated liquid motion are expressed as follows.

$$Fb = (4/3)\pi R_I^3(\rho_M - \rho_I)g \tag{4}$$

$$\begin{aligned} Fd &= (1/2)Cd_M\pi R_I^2\rho_M\cdot dZ/dt\cdot|\,dZ/dt\,| \\ &= 6\pi R\mu_M\cdot dZ/dt \end{aligned} \tag{5}$$

$$Ff = (1/2)\cdot(4/3)\pi R_I^3\rho_M\cdot d^2Z/dt^2 \tag{6}$$

From Fig. 1(a), the following equations are obtained.

$$\sin^2\theta_c = (2R_I+S-Z)(S+Z)/(R_I+S)^2,\quad \cos\theta_c = (R_I-Z)/(R_I+S) \tag{7}$$

The inclusion motion across the interface is expressed as follows.

$$d^2Z^*/dt^{*2}=2(\rho_M-\rho_I)/(\rho_M+2\rho_I)-3\alpha r_1\cdot Ar_1(Z^*,S^*) \\ -(2/\gamma r_1)\cdot\Gamma r_1(Z^*,S^*)\cdot dZ^*/dt^*-(9/\beta d_1)\cdot dZ^*/dt^* \quad (8)$$

Here, superscript* shows the dimensionless form by the respective length R_I and the time $(R_I/g)^{(1/2)}$. Eq. (8) is used in the range $0\leqq Z^*\leqq 2$ $(0\leqq Z\leqq 2R_I)$. Dimensionless parameters αr_1, $Ar_1(Z^*,S^*)$, βd_1, γr_1, $\Gamma r_1(Z^*,S^*)$ are expressed as follows.

$$\alpha r_1=\sigma_{MS}/\{R_I^2(\rho_M+2\rho_I)g\} \quad (9)$$
$$Ar_1(Z^*,S^*)=(2+S^*-Z^*)(S^*+Z^*)/(1+S^*)^3 \quad (10)$$
$$\beta d_1=(R_I^3g)^{(1/2)}/\{\mu_M/(\rho_M+2\rho_I)\} \quad (11)$$
$$\gamma r_1=(R_I^3g)^{(1/2)}/\{\mu_S/(\rho_M+2\rho_I)\} \quad (12)$$
$$\Gamma r_1(Z^*,S^*)=[(3/2)\{1/(1+2S^*)-1/(1+4S^*)\}]\cdot[1-\{(1-Z^*)/(1+S^*)\}^3] \quad (13)$$

From Eq. (1), the flow-out velocity U from the film is expressed as follows.

$$U=-1/(r\cdot\sin\theta)\cdot\partial\psi/\partial r=dZ/dt\cdot\sin\theta_c \quad (14)$$

From Fig. 1(a), the film surface area δ is expressed as follows.

$$\delta=\int(2\pi R_I\sin\theta)R_I d\theta=2\pi R_I^2(S+Z)/(R_I+S) \quad (15)$$

The equation of continuity of film flow is expressed as follows.

$$S\delta-U(2\pi R_I\sin\theta_c)Sdt=(S+dS)(\delta+d\delta) \quad (16)$$

Here, dS, dZ and $d\delta$ are the small varieties of S, Z and δ corresponding to the small time dt. Rearranging by substituting Eqs. (14) and (15) into Eq. (16), considering $R_I \gg S$ and neglecting the second order in dS and dZ, the dimensionless equation of continuity is obtained as follows [6].

$$dS^*/dt^*=[-dZ^*/dt^*\cdot(2-Z^*)(S^*+Z^*)\cdot S^*-S^*\cdot dZ^*/dt^*]/(2S^*+Z^*) \quad (17)$$

Finally, the displacement of the inclusion and the film thickness can be obtained as a function of the time by solving Eqs. (8) and (17) simultaneously under the specific initial conditions.

2.2.2 Inclusion without steel film

In this section, the dynamic force on inclusion without steel film is described. Considering the change of the interfacial energy Er accompanying the transfer of an inclusion from the interior of the steel to the slag-steel interface, the rebound force Fr is obtained as follows [3].

$$Er=-\pi(2R_IZ-Z^2)\sigma_{MS}+2\pi R_IZ\sigma_{SI}+2\pi R_I(2R_I-Z)\sigma_{IM} \quad (18)$$
$$Fr=dEr/dZ=2\pi R_I\sigma_{MS}\cdot Ar_2(Z^*) \quad (19)$$

The buoyancy force Fb, the drag force Fd and the fluid added mass force Ff due to the accelerated liquid motion are expressed as follows.

$$Fb=(4/3)\pi R_I^3\rho_S\cdot\Delta bf_2(Z^*)g-(4/3)\pi R_I^3\rho_I g \quad (20)$$
$$Fd=(1/2)Cd_S\pi(2R_IZ-Z^2)\rho_S\cdot dZ/dt\cdot|dZ/dt|+(1/2)Cd_M\pi(R_I-Z)^2\rho_M\cdot dZ/dt\cdot|dZ/dt| \\ =6\pi R\mu_S\cdot Bd_2(Z^*)\cdot dZ/dt \quad (21)$$
$$Ff=(1/2)\cdot(4/3)\pi R_I^3\rho_S\cdot\Delta bf_2(Z^*)\cdot d^2Z/dt^2 \quad (22)$$

The inclusion motion across the interface is expressed as follows.

$$d^2Z^*/dt^{*2}=2(\rho_S\Delta bf_2(Z^*)-\rho_I)/(\rho_S\Delta bf_2(Z^*)+2\rho_I) \\ -3\alpha r_2(Z^*)\cdot Ar_2(Z^*)-(9/\beta d_2(Z^*))\cdot Bd_2(Z^*)\cdot dZ^*/dt^* \quad (23)$$

Eq. (23) is also used in the range $0\leqq Z^*\leqq 2$ $(0\leqq Z\leqq 2R_I)$. Dimensionless parameters $\alpha r_2(Z^*)$, $Ar_2(Z^*)$, $\beta d_2(Z^*)$, $Bd_2(Z^*)$, $\Delta bf_2(Z^*)$ are expressed as follows.

$$\alpha r_2(Z^*)=\sigma_{MS}/\{R_I^2(\rho_S\cdot\Delta bf_2(Z^*)+2\rho_I)g\} \quad (24)$$
$$Ar_2(Z^*)=Z^*-1-\cos\theta_{IMS}, \quad \cos\theta_{IMS}=(\sigma_{IM}-\sigma_{SI})/\sigma_{MS} \quad (25)$$
$$\beta d_2(Z^*)=(R_I^3g)^{(1/2)}/\{\mu_S/(\rho_S\cdot\Delta bf_2(Z^*)+2\rho_I)\} \quad (26)$$
$$Bd_2(Z^*)=(\mu_M/\mu_S-1)\cdot Z^{*2}-2(\mu_M/\mu_S-1)\cdot Z^*+\mu_M/\mu_S \text{ for } 0\leqq Z^*\leqq 1, \quad Bd_2(Z^*)=1 \text{ for } Z^*\geqq 1 \quad (27)$$
$$\Delta bf_2(Z^*)=(1/4)(\rho_M/\rho_S-1)\cdot Z^{*3}-(3/4)(\rho_M/\rho_S-1)\cdot Z^{*2}+\rho_M/\rho_S \quad (28)$$

The displacement of the inclusion can be obtained as a function of the time by solving Eq. (23).

3. Comparison of Theory with Previous Experiments

In previous simulation-experiments [7~9], detailed assimilation behavior of the Al_2O_3 inclusion on the graphite plate by the slag was observed using a high-speed camera. The Al_2O_3 inclusion radius R_I was 1mm. The formation of steel film could be neglected because of $u_{I(0)}=0$, namely, $Re_{I(0)}=0$. The comparison of the calculated values with the experimental data for $u_{I(AV)}$ in a single Al_2O_3 inclusion is shown in Table 1. Here, the values of physical properties were determined from the estimate methods [12], which were proposed by one of the authors. Table 1 shows that the numerical results qualitatively agree with the experimental data. Furthermore, these previous experiments ($0.207 \leqq \mu_S \leqq 15.726$ poise, $0.416 \leqq \cos\theta_{IMS} \leqq 0.839$ and $u_{I(0)}=0$) revealed that the rate of inclusion assimilation was predominated by slag viscosity μ_S and wettability $\cos\theta_{IMS}$. The difference between the experimental and theoretical results is small. The similarity supported the assumption that the inclusion elimination could be predicted approximately using this simple theoretical model.

Table 1. The comparison of calculated values with the experimental data for $u_{I(AV)}$.

No.	Slag Melts	Chemical compositions of Slag Melts (−) $XSiO_2$	XAl_2O_3	$XCaF_2$	XMgO	XCaO	XNa_2O	ρ_S (g/cm³)	μ_S (poise)	σ_S (dyn/cm)	θ_{SI} (deg)	σ_{SI} (dyn/cm)	$\cos\theta_{IGS}$ (−)	$u_{I(AV)}$ (cm/s) Exp.	Cal.	Error (−)
8) (SAF21)	SiO_2-Al_2O_3-CaF_2-CaO 1823K	0.147	0.111	0.041		0.697	0.004	2.74	0.207	444	33.0	377	0.839	70	67.1	-0.043
9) (SAF22)	SiO_2-Al_2O_3-CaF_2-CaO-Na_2O 1823K	0.057	0.119	0.096		0.641	0.087	2.66	0.50	417	42.2	441	0.741	51	60.4	0.156
		0.561	0.167	0.017		0.189	0.066	2.40	15.726	371	85.3	720	0.819	1.7	1.3	-0.308
7) (SAF23)	SiO_2-Al_2O_3-CaF_2-MgO-CaO 1823K	0.503	0.137	0.072	0.069	0.218		2.49	2.762	377	65.4	593	0.416	7	6.7	-0.045

Conditions: (Gas); Ar, (Inclusion); Al_2O_3 ···· d_I = 1.0mm $\quad \sigma_{SI}=\sigma_I-\sigma_S\cdot\cos\theta_{SI}$
ρ_I = 3.99 g/cm³, σ_I = 750 dyn/cm $\quad \cos\theta_{IGS}=(\sigma_I-\sigma_{SI})/\sigma_S$

4. Numerical Results and Discussion

4.1 Calculation conditions

The preliminary approach towards an interface takes place under the influence of buoyancy or of convection currents. Here, only the influence of buoyancy is considered. Therefore, the initial displacement of the inclusion is zero and the initial velocity of the inclusion $u_{I(0)}$ is $u_{I(0)t}$, where $u_{I(0)t}$ is the terminal velocity of the inclusion and is equal to $(2/9)R_I^2(\rho_M-\rho_I)g/\mu_M$. The steel film can be formed in the range $d_I > 175\mu m$, when $u_{I(0)}=u_{I(0)t}$. This corresponds to the region $Re_{I(0)} \geqq 1$. The initial film thickness $S_{(0)}$ is selected to be $2\times10^{-3}R_I$. Since the rupture thickness of steel film seems to be less than about $0.1\mu m$, S_C is assumed to be $1\times10^{-3}R_I$ [5]. In order to estimate the influence of μ_S, $\cos\theta_{IMS}$ and d_I on inclusion elimination behavior, the calculation conditions for steel(pure iron)-slag(SAF9, SAF10, SAF11)-inclusion(INC1;Al_2O_3) systems and steel(pure iron)-slag(SAF11)-inclusion(INC1;Al_2O_3, INC2;Al_2O_3-SiO_2-FeO-TiO_2, INC3;Al_2O_3-SiO_2-TiO_2) systems are presented in Table 2 and Table 3, respectively.

Table 2. Calculation conditions in Eqs. (8), (17) or (23); Calculated values of ρ_S, μ_S, σ_S, θ_{MS}, σ_{MS}, θ_{SI} and $\cos\theta_{IMS}$ for steel(pure iron)-slag(SAF9, SAF10, SAF11)-inclusion(INC1;Al_2O_3) systems.

No.	Slag Melts	Chemical composition of Slag Melts. (−) $XSiO_2$	XAl_2O_3	$XCaF_2$	XMgO	XCaO	XLi_2O	XNa_2O	ρ_S (g/cm³)	μ_S (poise)	σ_S (dyn/cm)	θ_{MS} (deg)	σ_{MS} (dyn/cm)	θ_{SI} (deg)	$\cos\theta_{IMS}$ (−)
11) (SAF9)	SiO_2-Al_2O_3-CaF_2-MgO-CaO-Na_2O 1823K	0.442	0.039	0.033	0.038	0.372		0.076	2.54	1.779	379	49.3	1389	37.0	0.761
		0.429	0.054	0.080	0.019	0.373		0.045	2.56	1.005	371	49.7	1395	36.2	0.755
		0.447	0.045	0.125	0.018	0.285		0.080	2.50	0.546	337	49.7	1412	34.3	0.732
12) (SAF10)	SiO_2-Al_2O_3-CaF_2-MgO-CaO-(Li_2O)-Na_2O 1823K	0.419	0.043	0.145	0.038	0.257		0.098	2.50	0.363	327	48.1	1409	28.4	0.739
		0.389	0.043	0.133	0.039	0.253	0.041	0.102	2.47	0.332	337	47.4	1400	30.2	0.747
		0.358	0.044	0.144	0.138	0.213		0.103	2.51	0.295	321	48.3	1413	23.9	0.742
		0.292	0.038	0.128	0.110	0.168	0.162	0.102	2.39	0.134	352	46.3	1387	32.8	0.757
(SAF11)	SiO_2-Al_2O_3-CaF_2-MgO-CaO 1823K	0.197	0.070	0.045	0.132	0.556			2.75	0.223	423	57.6	1425	33.1	0.778

Conditions: (Metal); Pure iron, (Inclusion); Al_2O_3.
σ_M = 1606 dyn/cm, ρ_M = 7.00 g/cm³, μ_M = 0.06 poise.
ρ_I = 3.99 g/cm³, θ_{IM} = 118 deg.
$\sigma_{MS}=[\sigma_M^2+\sigma_S^2-2\sigma_M\cdot\sigma_S\cdot\cos\theta_{MS}]^{1/2}$.
$\cos\theta_{IMS}=(\sigma_{IM}-\sigma_{SI})/\sigma_{MS}=(\sigma_S\cdot\cos\theta_{SI}-\sigma_M\cdot\cos\theta_{IM})/\sigma_{MS}$.

Table 3. Calculation conditions in Eqs. (8), (17) or (23); Calculated values of ρ_I, θ_{IM}, θ_{SI} and $\cos\theta_{IMS}$ for steel(pure iron)-slag(SAF11)-inclusion(INC1;Al_2O_3, INC2;Al_2O_3-SiO_2-FeO-TiO_2, INC3;Al_2O_3-SiO_2-TiO_2) systems.

No.	Inclusions	Chemical compositions of Inclusions (−) XAl_2O_3	$XSiO_2$	XFeO	$XTiO_2$	ρ_I (g/cm³)	θ_{IM} (deg)	θ_{SI} (deg)	$\cos\theta_{IMS}$ (−)
(INC1)	Al_2O_3 1823K	1.000				3.99	118	33.1	0.778
(INC2)	Al_2O_3-SiO_2-FeO-TiO_2	0.494	0.336	0.139	0.031	3.67	110	32	0.637
		0.447	0.379	0.102	0.071	3.57	105	22	0.567
	1823K	0.350	0.475	0.049	0.127	3.40	99	18	0.459
(INC3)	Al_2O_3-SiO_2-FeO-TiO_2	0.205	0.697	0.010	0.088	3.07	24	16	-0.744
		0.417	0.472	0.011	0.100	3.38	22	20	-0.766
	1823K	0.185	0.627	0.010	0.179	3.15	12	30	-0.845

Conditions : (Slag Melt); SAF11, (Metal); Pure Iron.
ρ_S=2.75 g/cm³, μ_S=0.223 poise, σ_S=423 dyn/cm
ρ_M=7.00 g/cm³, μ_M=0.06 poise, σ_M=1606 dyn/cm
θ_{MS}=57.6 deg, σ_{MS}=1425 dyn/cm
$\sigma_{MS}=[\sigma_M^2+\sigma_S^2-2\sigma_M\cdot\sigma_S\cdot\cos\theta_{MS}]^{1/2}$
$\cos\theta_{IMS}=(\sigma_{IM}-\sigma_{SI})/\sigma_{MS}=(\sigma_S\cdot\cos\theta_{SI}-\sigma_M\cdot\cos\theta_{IM})/\sigma_{MS}$

4.2 Displacement of inclusion and thickness of steel film

The relation of Z to t at μ_S=1.779 poise, $\cos\theta_{IMS}$=0.761 and $u_{I(0)}=u_{I(0)t}$ for various d_I is shown in Fig. 2. Fig. 2 shows that for inclusions ③,④,⑤ larger than 100 μm in diameter, Z increases in proportion to time until float-out, and that for inclusions ①,② smaller than 50 μm in diameter, Z increases in proportion to time until Z reaches its maximum value, where Z is 1.76～1.88R_I, then decreases gradually with time. 'Pass' indicates the inclusion passing out ($Z=2R_I$) and 'Stay' indicates the inclusion stopping once ($u_I=dZ/dt\leqq 0$). Furthermore, for inclusion ⑤ larger than 200 μm in diameter with film formation, the film rupture delays the float-out time for 0.370×10^{-4}s. The arrow sign in Fig. 2 indicates the film rupture at $S_C=1\times10^{-3}R_I$.

The relation of Z to t at μ_S=0.223 poise, $\cos\theta_{IMS}$=-0.845 and $u_{I(0)}=u_{I(0)t}$ is shown in Fig. 3. Fig. 3 shows that for all size inclusions ②,③,④,⑤, Z changes according to the damped oscillation across the interface, where Z at its maximum value is about 0.30R_I, and therefore there is little chance of float-out. 'Osc.' indicates the inclusion moving according to the damped oscillation. Furthermore, for inclusion ⑤ larger than 200 μm in diameter with film formation, the film rupture delays the start time of the damped oscillation for 0.255×10^{-4}s. The arrow sign in Fig. 3 also indicates the film rupture at $S_C=1\times10^{-3}R_I$.

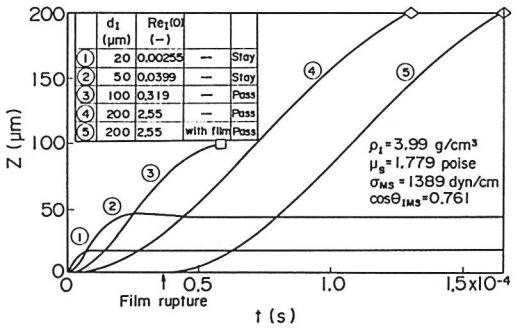

Fig. 2. The relation of inclusion displacement Z to time t at μ_S=1.779 poise, $\cos\theta_{IMS}$ =0.761 and $u_{I(0)}=u_{I(0)t}$; steel(pure iron) -slag(SAF9)-inclusion(INC1;Al_2O_3) system.

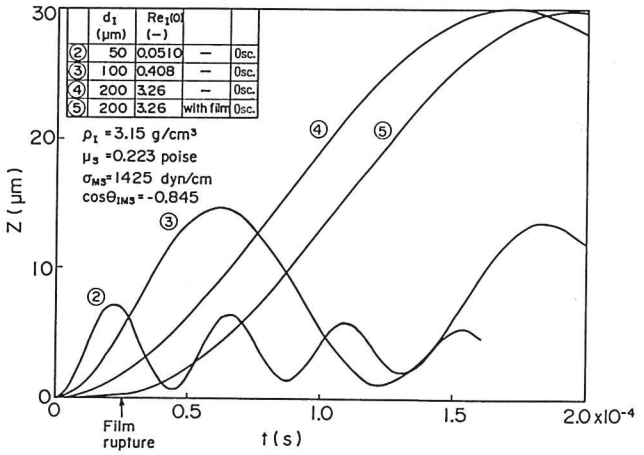

Fig. 3. The relation of inclusion displacement Z to time t at μ_S=0.223 poise, $\cos\theta_{IMS}$=-0.845 and $u_{I(0)}=u_{I(0)t}$; steel(pure iron)-slag(SAF11 -inclusion(INC3;Al_2O_3-SiO_2-TiO_2) system.

4.3 Region of inclusion elimination

Figs. 4 and 5 show the region where the inclusion is eliminated for various μ_S and $\cos\theta_{IMS}$. The open mark indicates the inclusion float-out region. The closed mark indicates 'Stay' or 'Damped oscillation' region. The influence of μ_S and $\cos\theta_{IMS}$ on inclusion elimination were estimated numerically. Consequently, it was found that the inclusion was not eliminated easily if $\mu_S>1.005$ poise, $d_I<50\,\mu$m or $\cos\theta_{IMS}<0$. Especially, inclusion INC3;Al_2O_3-SiO_2-TiO_2 never floats out, because of wettability $\cos\theta_{IMS}<0$.

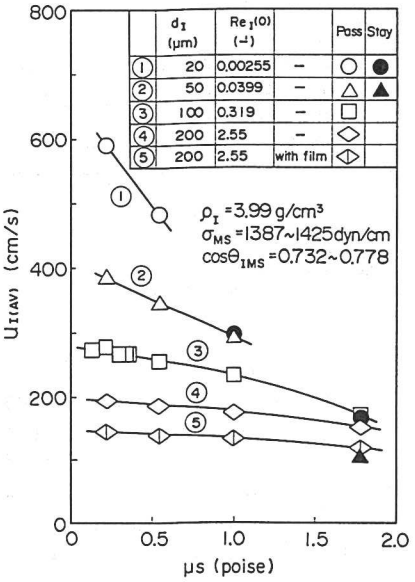

Fig. 4. The influence of μ_S on $u_{I(AV)}$ for steel (pure iron)-slag (SAF9, SAF10, SAF11)-inclusion (INC1; Al_2O_3) systems.

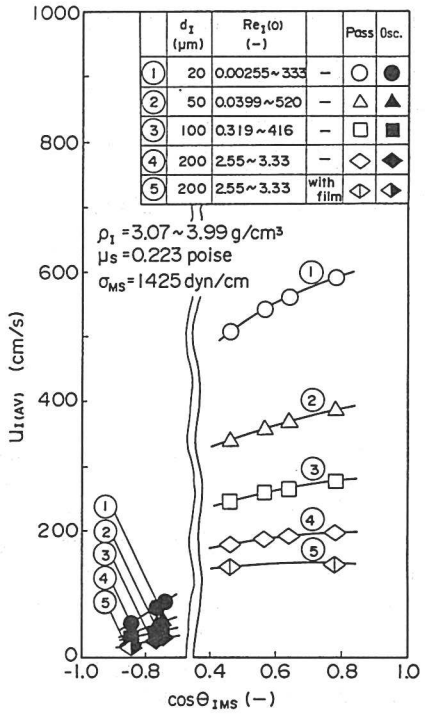

Fig. 5. The influence of $\cos\theta_{IMS}$ on $u_{I(AV)}$ for steel (pure iron)-slag (SAF11)-inclusion (INC1; Al_2O_3, INC2; Al_2O_3-SiO_2-FeO-TiO_2, INC3; Al_2O_3-SiO_2-TiO_2) systems.

5. Conclusion

(1) A theoretical analysis based on an effective model has been developed by considering wettability and slag viscosity. The critical condition of inclusion elimination was obtained quantitatively.

(2) Comparing the numerical results with previous simulation-experimental results, the validity of the theoretical model was confirmed.

Nomenclature

d_I : inclusion diameter $=2R_I$
R_I : inclusion radius
Re_I : Reynolds number $\equiv \rho_I \cdot u_I \cdot 2R_I / \mu_M$
S : steel film thickness
S_c : rupture thickness of steel film
t : time
U : steel flow-out velocity from film
u_I : rising velocity of inclusion $\equiv dZ/dt$
Z : inclusion displacement
σ : surface tension, interfacial tension
μ : viscosity
ρ : density

Subscript and superscripts

(0), (AV) : initial value, average value, respectively
F, G, I, M, S : film, gas, inclusion, metal, slag, respectively
ij : i-j interface
* : dimensionless form by R or $(R/g)^{(1/2)}$
$dZ/dt \equiv (R_I g)^{(1/2)} \cdot dZ^*/dt^*$, $d^2Z/dt^2 \equiv g \cdot d^2Z^*/dt^{*2}$

References

1) H. M. Princen: J. Colloid Sci., 18 (1963), p. 178
2) Y. G. Gurevitch: Izv. VUZ Chern. Metall., (1968) 8, p. 5
3) T. A. Engh, H. Sandberg, A. Hultkvist and L. G. Norberg: Scand. J. Metall., 1 (1972), p. 103
4) L. I. Krupman and Y. G. Yaroslavtesev: Izv. AN SSSR. Met., (1977) 5, p. 48
5) P. V. Ribound and M. Olette: Proc. 7th ICVM, 1982, Tokyo, Japan, p. 879
6) H. Hashimoto and S. Kawano: JSME Int. J. Ser. 2, 33 (1990) 4, p. 729
7) K. P. Bziava and V. V. Averin: Izv. AN SSSR. Met., (1972) 2, p. 18
8) L. I. Krupman, Y. G. Yaroslavtesev, V. V. Averin and K. P. Bziava: Izv. AN SSSR. Met., (1977) 3, p. 21
9) L. I. Krupman and Y. G. Yaroslavtesev: Stal', (1982) 8, p. 37
10) A. P. Manyugin, G. A. Sokolov, A. G. Sergeev and E. A. Tonkikh: Izv. VUZ Chern. Metall., (1980) 9, p. 36
11) K. C. Mills, A. Olusanya, R. Brooks, R. Morrell and S. Bagha: Ironmaking Steelmaking, 15 (1988), p. 257
12) K. Nakajima, K. Yasumoto, K. Nakai and Z. Morita: Proc. Int. Symp. Developments in Ladel Steelmaking and Continuous Casting, 1990, Hamilton, Canada, p. 338